VALIDATION CASE RESULTS FOR 2D AND 3D MHD SIMULATIONS

Ming-Jiu Ni[1, 3], Ramakanth Munipalli[2], Neil B Morley[1], Peter Huang[2], Mohamed A. Abdou[1]

[1]*MAE Dept., University of California, Los Angeles, CA, 90095-1597, Email: mjni@ucla.edu*
[2]*HyperComp Inc., Westlake Village, CA, 91362-7140*
[3]*Graduate University of Chinese Academy of Sciences, Beijing, 100049, China*

*A consistent and conservative scheme designed by Ni et al. for the simulation of MHD flows with low magnetic Reynolds number has been implemented into a 3D parallel code of HIMAG based on solving the electrical potential equation. The scheme and code are developed on an unstructured collocated mesh, on which velocity (**u**), pressure (p), and electrical potential (φ) are located in the cell center, while current fluxes are located on the cell faces. The calculation of current fluxes is performed using a conservative scheme, which is consistent with the discretization scheme for the solution of electrical potential Poisson equation. The Lorentz force is calculated at cell centers based on a conservative formula or a conservation interpolation of the current density. We validate the numerical methods, and the parallel code by simulating 2D fully developed MHD flows with analytical solutions existed and 3D MHD flows with experimental data available. The validation cases are conducted with Hartmann number from 100 to 10^4 on rectangular grids and/or unstructured hexahedral and prism grids.*

I. INTRODUCTION

The simulation of magnetohydrodynamic (MHD) flows at high Hartmann numbers has been a topic of great interest in the development of a fusion reactor blanket[3, 4]. The self-cooled liquid-metal blanket[5] and dual coolant lead lithium (DCLL) blanket[6] use liquid lithium or the eutectic alloy Pb-17Li as the coolant and breeding material. To design self-cooled liquid metal or DCLL blankets for fusion reactors, one must have a predictive capability for MHD flows at high Hartmann numbers[7].

MHD in duct flows has been extensively studied by asymptotic theory and numerical simulation[8-11]. The square of the Hartmann number *Ha* is the ratio between the electromagnetic and the viscous forces. It is a measure of the magnetic field strength for a given fluid in a duct of a given scale. The thickness of the Hartmann layers on all walls normal to field scales with Ha^{-1} and so are very thin for high Ha flows. The side layers on all walls parallel to the magnetic field scale with $Ha^{-1/2}$ and are much thicker than the Hartmann layers at high Hartmann numbers. Resolving these layers for conditions relevant to fusion requires a very fine mesh. For unsteady flows, the time step is proportional to the smallest grid size, making the cost for MHD at high Hartmann numbers is very high.

The flow of electrically conducting fluid under the influence of an external magnetic field is governed by the following Navier-Stokes equation and continuity equation, which represent the conservation of momentum and mass:

$$\frac{\partial \boldsymbol{u}}{\partial t} + \boldsymbol{u}\cdot\nabla\boldsymbol{u} = -\nabla p + \frac{1}{Re}\nabla^2\boldsymbol{u} + N(\boldsymbol{J}\times\boldsymbol{B}) \qquad (1)$$

$$\nabla\cdot\boldsymbol{u} = 0 \qquad (2)$$

Here $\boldsymbol{u}$, p are the non-dimensional velocity vector and kinetic pressure scaled with v_0 and ρv_0^2 respectively. With L defined as characteristic length, $Re = v_0 L/\eta$ is the Reynolds number, $Ha = LB_0\sqrt{\sigma/\rho\eta}$ is the Hartmann number, and $N = Ha^2/Re$ is the interaction parameter. $\boldsymbol{J}$ represents the current density, and $\boldsymbol{B}$ is the applied magnetic field, scaled with $\sigma v_0 B_0$ and B_0 respectively. Also we define the magnetic Reynolds number here as $Re_m = \mu\sigma L v_0$, where η and σ are the fluid viscosity and conductivity respectively. μ is the magnetic permeability of the fluid and the walls, and ρ is the density of the fluid. The term $N(\boldsymbol{J}\times\boldsymbol{B})$ is the Lorentz force, which is a volume force in a non-conservative form in the momentum equation Eq. (1).

For low magnetic Reynolds numbers, the flow of electrically conducting fluid under the influence of an external magnetic field with negligible induced field, the current density can be calculated through Ohm's law[12, 13]:

$$\boldsymbol{J} = -\nabla\varphi + \boldsymbol{u}\times\boldsymbol{B} \qquad (3)$$

The current density is conservative, such that:

$$\nabla\cdot\boldsymbol{J} = 0 \qquad (4)$$

From Eqs. (3) and (4), we can get the electrical scalar potential equation as:

$$\nabla \cdot (\nabla \varphi) = \nabla \cdot (\boldsymbol{u} \times \boldsymbol{B}) \quad (5)$$

For incompressible MHD flow, the numerical scheme used by Sterl[14] on a uniform staggered rectangular grid system is limited to low Hartmann numbers and simple geometries. The scheme used by Leboucher[15-17] on a nonuniform fully staggered rectangular grid system is limited to simple geometries and uni-directional applied magnetic field. The schemes used by Mistrangelo[18], Piazza[19], and Aleksandrova et al. [20] on a collocated grid system are not current density conservative, which may have problems getting a conservative current a high Hartmann number MHD flow.

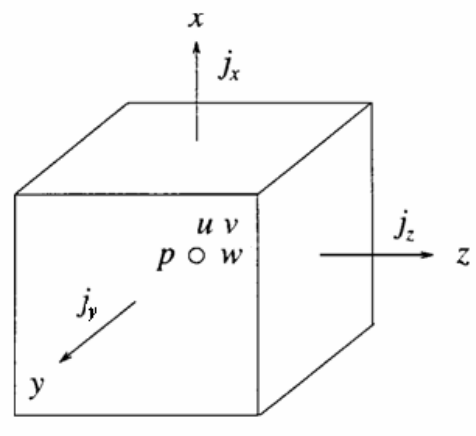

(a) A Rectangular Collocated Grid

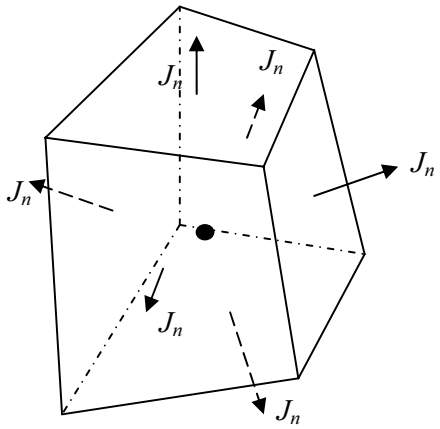

(b) An Unstructured Collocated Grid

Figure 1: Illustration of Computation Cell for MHD

A consistent and conservative scheme or a current density conservative scheme is developed on a rectangular collocated mesh[1] as shown in Fig. 1a and on an arbitrary unstructured mesh[2] as shown in Fig. 1b. In this collocated grid, velocity ($\boldsymbol{u}$), pressure (p), and electrical potential (φ) are located in a grid center, while current fluxes are located on cell faces. The scheme used to calculate the current flux should be "consistent" with the scheme used in the electrical potential Poisson equation. A consistent scheme is necessary to get divergence-free current fluxes on cell faces of a control volume. The Lorentz force is calculated based on the conservative current density fluxes using a conservative formulation of the force or a conservative interpolation of current densities to the cell centers. When the applied magnetic field is constant, the total momentum contribution from the Lorentz force calculated from the consistent and conservative scheme is zero or just dependent on the boundary conditions.

We will validate that the consistent and conservative scheme has a good resolution at the side layers and the Hartmann layers, even at high Hartmann numbers. In this paper, a general second-order projection method[21] is used to conduct the simulations of incompressible Navier-Stokes equations.

II. Validation of Consistent and Conservative Scheme

There exist some exact solutions for fully developed incompressible laminar flows in ducts with transverse magnetic fields, such as (1) Shercliff's solution for rectangular ducts with non-conducting walls and the field perpendicular to one side[9]; (2) Hunt's solution for rectangular ducts with two non-conductive side walls and two conductive Hartmann walls[10]. These two solutions will be used in this paper to verify our methods and code mentioned above. Hunt's formula has been reformulated in Ref. 1 for the sake of numerical calculation using computer code at high Hartmann number. Considering that Shercliff's case is a special case of Hunt's case, the reformulated Hunt's formula can also be used to get the exact solution for Shercliff's case.

II.A. Shercliff's Case

The Shercliff's case with all of the walls insulated is simulated. We present some preliminary results from a fully developed flow calculation at Ha = 1000 and Re = 10, a dimensionless mass flow rate of 4 and a pressure gradient from Shercliff's solution (with appropriate numerical implementation) of -102.88.

We present a comparison between the Hartmann layer and side layer structure from Shercliff's analysis with the present conservative/consistent scheme solved on both a coarse (33×33 nonuniform cells) and fine mesh (66×66 nonuniform cells) solutions in Fig. 2a and 2b. As can be seen the comparison is better than 0.1% for the fine mesh case. The solution on the coarse mesh indicates an error of about 0.5% in mass flow rate and peak velocity with uniform convergence.

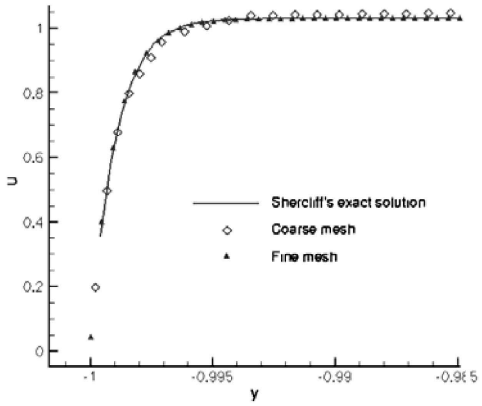

(a) Hartmann Layer

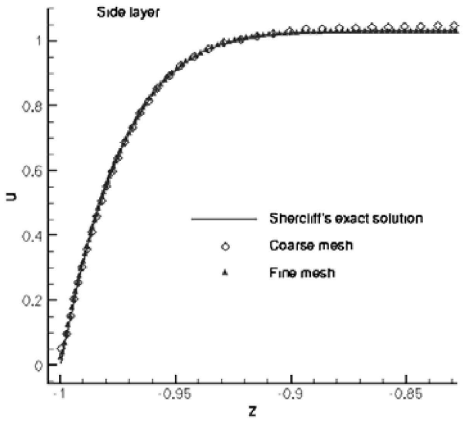

(b) Side Layer

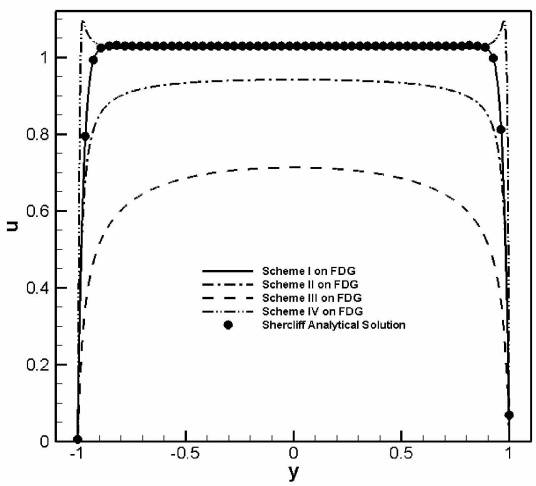

(c) Velocity distribution using different schemes

Figure 2: A comparison of numerical and exact solutions at *Ha* = 1000

Figure 2c shows the comparison between Shercliff's analytical results and numerical results for the fine mesh where we can see the velocity from the consistent and conservative scheme (labeled as Scheme I) matches the analytical result well., Various non-conservative schemes (labeled as Scheme II Scheme III and Scheme IV), which have similar features as in Refs. 18-20, either calculate lower velocities compared to the Shercliff's analytical result or give good results in the core flow but a non-physical velocity jump in the Hartmann layers. The comparison demonstrates a very good computational accuracy of the consistent and conservative scheme.

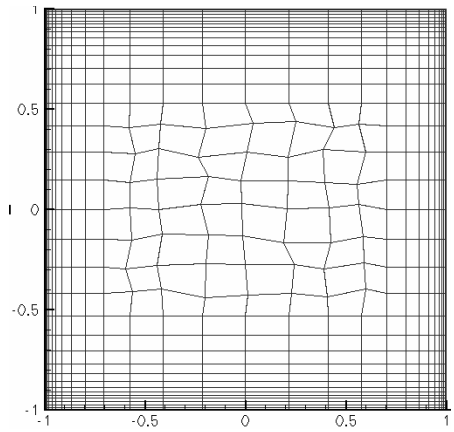

(a) An orthogonal mesh with core-perturbation

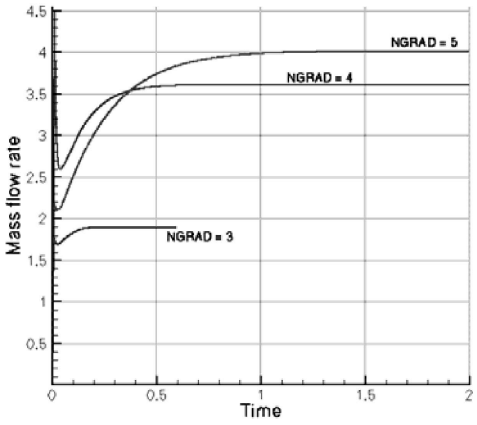

(b) Mass flow rate convergence (exact solution: Q = 4)

Figure 3: Shercliff's case with *Ha* = 300 on an orthogonal mesh with core-perturbation

We now consider a fully developed flow calculation on a generally orthogonal mesh, but with some core cell geometric perturbations (Fig. 3a) at *Ha* = 300 and *Re* = 10 with a pressure gradient of -31.67 specified which corresponds to a mass flow rate of 4 from Shercliff's solution. On the mesh of Fig. 3a, the consistent scheme is used to conduct the calculation of the current fluxes on

the cell faces, which meet the condition of the divergence free of the current density in a controlled volume. The Lorentz force is calculated based on the conservative formulation (which can conserve the momentum at an arbitrary mesh) represented as "NGRAD = 5", the simple interpolation (which is equivalent to the Scheme I in a rectangular grid and can conserve current density and the momentum only on a rectangular grid, but not on a skewed grid) represented as "NGRAD = 4", and the non-conservative scheme (which is equivalent to the nonconservative scheme II in a rectangular grid and cannot conserve the current density and momentum at any kind of mesh – Scheme II) represented as "NGRAD = 3" in Fig. 3b. Fig. 3b tells us the Lorentz force calculated based on the conservative formulation can be used to get an accurate result, which matches well with the analytical results on the skewed grids. However, the simple interpolation cannot get an accurate result for MHD even at *Ha* = 300; while the Lorentz force from the non-conservative scheme gives the value of flow rate with the most deviation from the actual result.

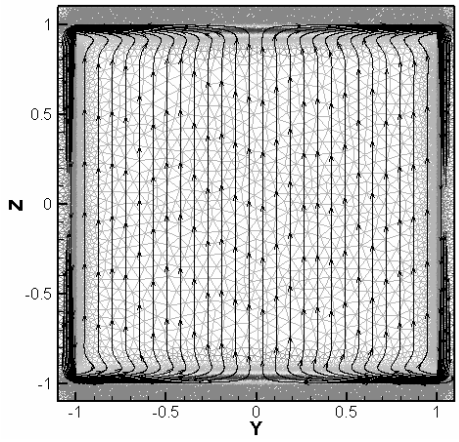

d: Triangular grids and current streamlines

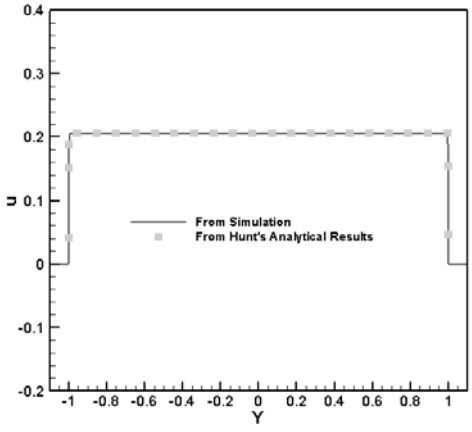

b: along the middle line normal to the Hartmann walls

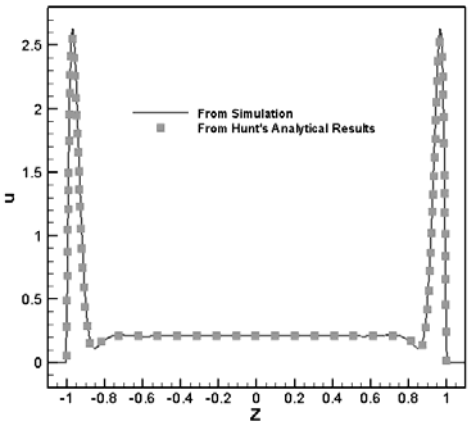

c: along the middle line normal to the side walls

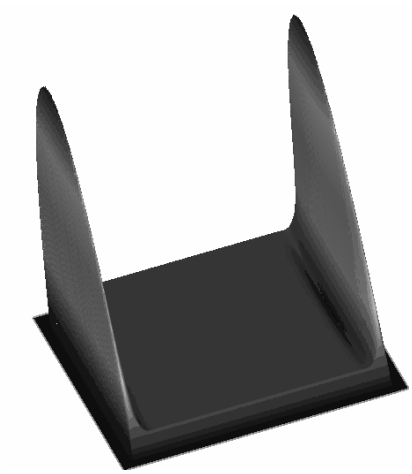

d: Velocity profile

Figure 4: Velocity profile and current streamlines for *Ha* = 1000 on a triangular mesh

Generally speaking, the current fluxes on the cell faces calculated using the consistent scheme are locally conservative in a control volume. The Lorentz force calculated based on the conservative current density fluxes is accurate. The consistent and conservative scheme on a collocated mesh can be employed to do simulations of MHD flows at high Hartmann numbers.

II.B. Hunt's Case

II.B.1. fully developed flow with Ha = 1000 on a triangular mesh

We now consider the fully developed flow in a square channel with *Re* = 10, *Ha* = 1000 for Hunt's case with the walls perpendicular to the applied magnetic field assumed to be conducting with a wall conductance ratio

c_w = 0.05, while those parallel to the applied magnetic field are electrically insulated.

The pressure gradient is given as a constant of -1000. A triangular mesh (shown in Fig. 4a,) is used in which the Hartmann layer region is resolved with cells having minimum size 1/(3*Ha)*, and maximum size 1/*Ha*. The grid also resolves the side layers with cells having a minimum size of $1/(3Ha^{1/2})$, and maximum size of $1/Ha^{1/2}$.

The comparison between the numerical results and the Hunt's analytical solution is illustrated in Fig. 4. Fig. 4b presents the comparison of the velocity along the center line normal to the Hartmann walls. The numerical results match well with the analytical results. Fig. 4c presents the comparison of the velocity along the center line normal to the side walls. The numerical results also match well with the analytical results. The velocity profile and the current distribution are given in Fig. 4d and 4a. Fig. 4a clearly shows the calculated current is conservative on the triangular mesh.

II.B.2. A case study of Ha = 10,000

We present here some observations on the calculation of *Ha* = 10,000 and Re = 1000 flow in a square duct. This is a large Hartmann number by the standard of full MHD simulations in 3D. We experimented with fully developed flow calculations in the cross section, as well as the three-dimensional developing flow situation. A channel of dimensions 2×2 is enclosed with walls with a thickness of 0.1 on all sides and resolved with a 67×67 cell non-uniform mesh having 4 cells in the Hartmann layer. The 3D mesh uses 20 mesh points over a length of 20 units. Pressure is held fixed at the exit plane, while the electric potential is held fixed at the inflow.

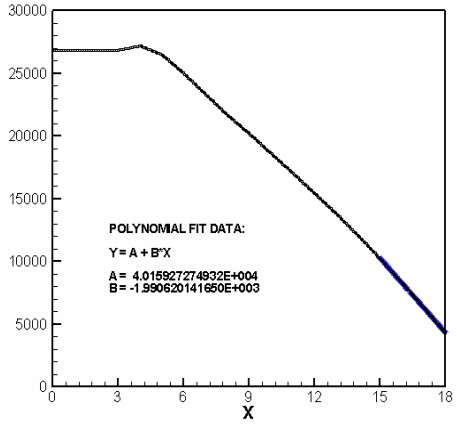

(a) Pressure Distribution

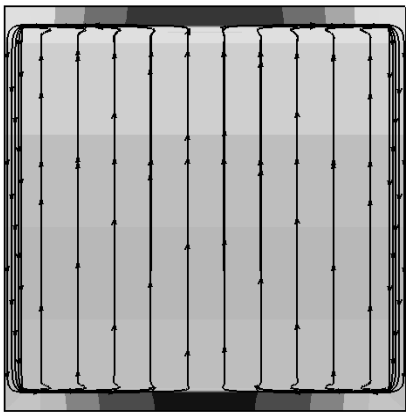

(b) Current Distribution

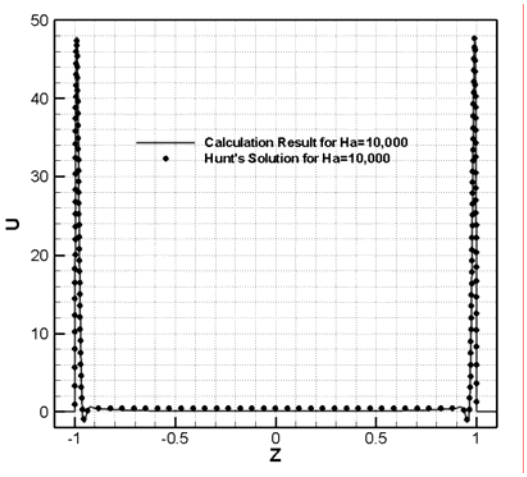

(c) Comparing with Hunt's Result

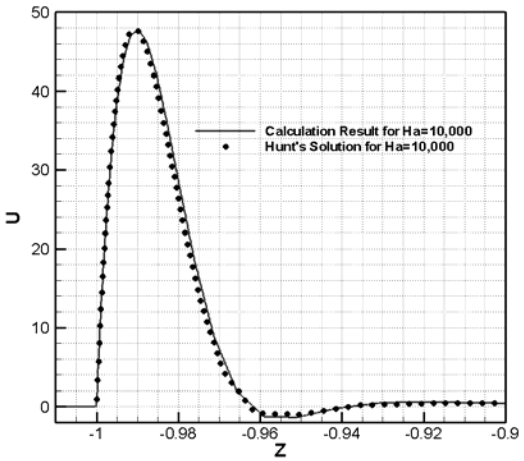

(d) with detailed view in side layer

Figure 5: Computed velocity profile and current lines for fully developed flow at Ha = 10,000 in a square duct

Again, the Hartmann walls are assumed to be conducting with a wall conductance ratio c_w = 0.05 and the side-walls are insulated. The magnetic field ramps up at x = 5.

We first present here results from the fully developed flow calculations. The fully developed flow simulations used a zero velocity at time t = 0, with a pressure gradient of -1000 to drive the flow. A mass flow rate value of 0.208 was observed in the fully developed flow situations. This compares well with Hunt's solution, which gives a flow rate of 0.203.

The 3-D case used a fixed mass flow rate of 4 at the inflow with a double parabola profile. This simulation is performed on a parallel cluster with 16 processors. The axial pressure distribution is illustrated in Fig. 5a with a pressure gradient of 1990.62 observed in the fully developed region, which is very close to the Hunt's analytical value of 1972.26. The convergent current distribution in the fully developed region is shown in Fig. 5b. Figure 5c gives the comparison between our results and Hunt's analytical results. Figure 5d zooms in the side layer. The numerical results from the consistent and conservative schemes on a collocated nonuniform grid match very well with Hunt's solution. The figure clearly shows the jets forming in the side layers.

II.B.3. Fully 3D simulation – comparison with an experiment for circular pipe flow

In a fusion blanket, 3-D effects are unavoidable and the flow profiles have a strong influence on heat transfer and corrosion rates. It is essential to validate the fully three-dimensional prediction of the present algorithm for a fully 3D MHD flow. While no exact analytical solution exists for 3D MHD flows of interest, experimental data from Refs. 22-23 for a MHD flows in a circular pipe with an axial distribution of the magnetic field varying with either rapid or slow spatial variations is used to compare with the computational results from the consistent and conservative scheme for MHD flows. The coordinate X is an axial distance from the edge of the magnet pole face, non-dimensionalized by the duct half-width.

In Ref. 22, two sets of experimental data are reported on the MHD flows in a circular pipe (Fig. 6a). We simulate the case with a higher Hartmann number and a higher interaction number MHD flow. The detailed parameters corresponding to this case are listed here. The radius is a = 0.0541 m. The working fluid has density ρ = 865 kg/m^3, electrical conductivity $\sigma = 2.86\times10^6/(\Omega m)$, viscosity $\eta = 8.2175\times10^{-4}$ $kg/(ms)$. The thickness of the wall is $t_w = 3.01\times10^{-3}$ m, and the conductivity of the wall is $\sigma_w = 1.39\times10^6/(\Omega.m)$. The conductance is c_w = 0.027. The applied magnetic field is a spatial variable with the maximum value B_{max} = 2.08 T. The inlet average velocity is U = 0.07 m/s. The non-dimensional parameters can be calculated as: Ha = 6640, N = 11061, Re = 3986.

The calculated results and experimental results are shown in Fig. 6. The solid curves in Fig. 6 are the results of the 3-D simulations done using the code of HIMAG[24] utilizing the consistent and conservative scheme for MHD flows. HIMAG is a parallel code mainly developed for MHD simulations at low magnetic Reynolds numbers.

Figure 6b presents the axial pressure gradient distribution along the side wall (perpendicular to the applied field) and along the top wall (tangent to the applied field). The pressure gradient in the Hartmann layer (along the side wall) is higher than it along the top wall in the fringing region. This difference of the axial pressure gradient between the side wall and the top wall is clearly shown in Fig. 6c. Figure 6c presents the pressure difference distributions between the pipe locations tangent to and perpendicular to the applied field for roughly the same conditions covered in Fig. 6b. In an ordinary fluid flow without a magnetic field, or in a fully developed flow inside a uniform field, the transverse pressure difference is zero. While the agreement between the experimental data and the 3-D code prediction is generally very good. The computed maximum pressure difference is slightly smaller than it from the experimental data, which shows that the computed axial pressure gradient at the Hartmann wall is likely smaller than that measured in the experiment.

Fig. 6d presents two axial velocity distributions from the numerical simulations compared with the experimental data. The lower data in the figure were taken at the duct centerline z = 0 (z = 1.0 at the duct wall). The upper data were taken at z = 0.9. The agreement between the experimental data and the simulation results is excellent. This figure shows dramatically the low velocity core region near the inlet to the magnet (lower data set) and the high velocity jet region near the walls (upper data set).

Figure 6e shows the 3D velocity profiles at different positions along the axial direction, which illustrates the transition of the MHD flow from inlet developing flow to outlet fully developed flows.

III. CONCLUSIONS

A consistent and conservative scheme designed for MHD flow simulations with low magnetic Reynolds numbers on an arbitrary collocated mesh has been implemented into a 3D parallel code – HIMAG. The consistent scheme can ensure the calculated current density fluxes on the cell faces of a control volume are divergence-free. These conservative current density fluxes are used to accurately calculate the Lorentz force at the cell centers based on the conservative formulation of the force or the conservative interpolation of the current density. The Lorentz force is conservative, which can ensure the total momentum contributed from the Lorentz

force is conservative when the applied magnetic field is spatially independent.

We validated this consistent and conservative scheme and the HIMAG code by simulating the fully developed MHD flows for which analytical solution exist, as well as 3D MHD flows with a spatially varying applied magnetic field for which experimental data are available. Our numerical results match well with the analytical solution and experimental data for a range of Hartmann numbers relevant to fusion conditions

Future work includes the continued validation and the application of this code to numerical simulations of 3D fusion blanket features with multiple materials and complex geometries such as flows with Flow Channel Inserts and manifold flow distribution regions

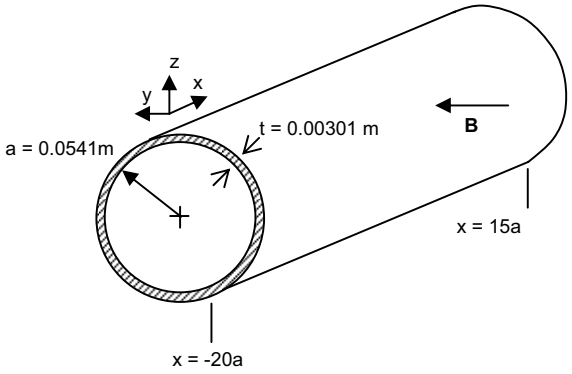

a. Sketch for computation geometry

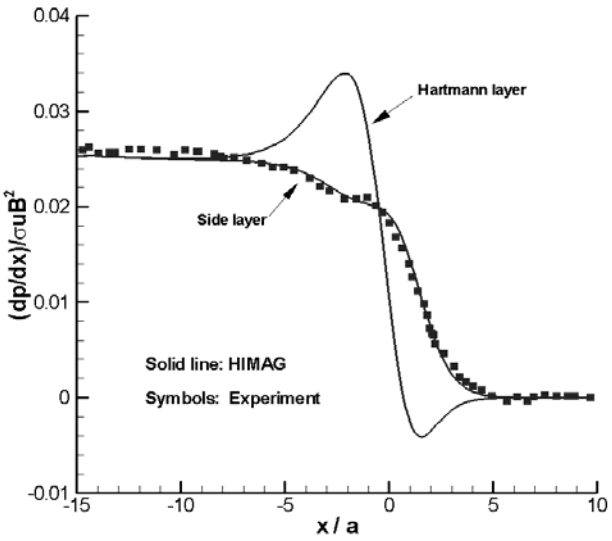

b: Pressure gradient comparison

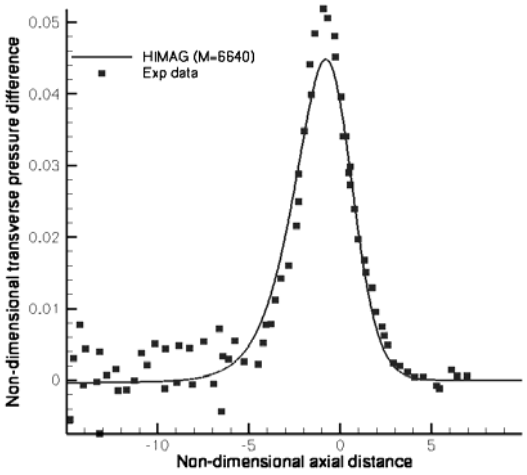

c: Transverse pressure difference

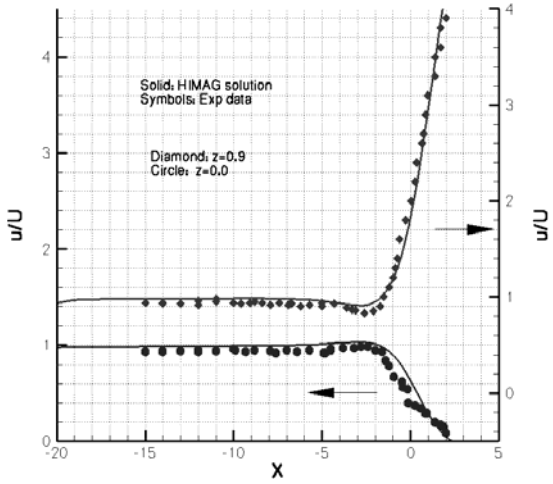

d: Velocity profiles

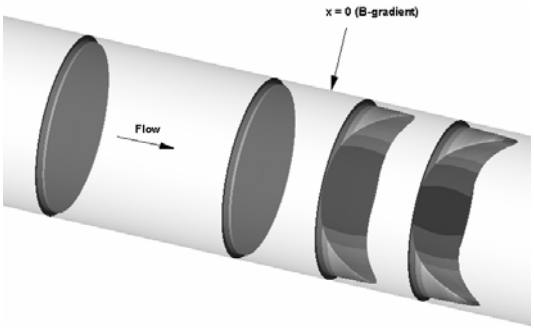

e: Velocity profiles along the channel

Figure 6: Fully 3D computations comparing with measurements

ACKNOWLEDGMENTS

The authors from UCLA acknowledge the support from the U.S. Department of Energy under Grant # DE-FG03-86ER52123, and the authors from HyperComp Inc. acknowledge the support from the U.S. Department of Energy under DOE SBIR Grant # DE-FG02-04ER83977. Leo Bühler is acknowledged for tips on the proper interpolation of experimental data from Ref. 22.

REFERENCES

1. M.-J. NI, R. MUNIPALLI, N.B. MORLEY, P.Y. HUANG and M.A. ABDOU, Consistent and Conservative Schemes for MHD with Low Magnetic Reynolds Number. Part I. on Structured Grid System, submitted to Journal of Computational Physics for Review
2. M.-J. NI, M.A. ABDOU, Consistent and Conservative Schemes for High Hartmann MHD with Low Magnetic Reynolds Number based on Conservative Formula of Lorentz Force. Part 2. On an Arbitrary Unstructured Collocated Grid System, to be submitted for review
3. M.A. ABDOU et al, On the Exploration of Innovative Concepts for Fusion Chamber Technology Fusion, Fusion Engineering and Design, **54**, 181 (2001)
4. N.B. MORLEY, S. SMOLENTSEV, R. MUNIPALLI, M.-J. NI, D. GAO, M.A. ABDOU, Progress on the Modeling of Liquid Metal, Free Surface, MHD Flows for Fusion Liquid Walls, Fusion Engineering Design, **72**, 3 (2004)
5. S. MALANG, et al., Self-Cooled Liquid-Metal Blanket Concept, Fusion Technology, **14**, 1343 (1988)
6. M.A. ABDOU, D. SZE, C. WONG, M. SAWAN, A. YING, N.B. MORLEY, S. MALANG, U.S. Plans and Strategy for ITER Blanket Testing, Fusion Science and Technology, **47**, 475 (2005)
7. L. BŮHLER, The Influence of Small Cracks in Insulating Coatings on MHD and Heat Transfer in Rectangular Ducts, Fusion Engineering and Design, **27**, 634 (1995)
8. J.A. SHERCLIFF, The Flow of Conducting Fluids in Circular Pipes under Transverse Magnetic Fields, Journal of Fluid Mechanics, **1**, 644 (1956)
9. J.A. SHERCLIFF, Steady Motion of Conducting Fluids in Pipes under Transverse Magnetic Fields, Proc. Cambridge Philosophical Society, **49**, 126 (1953)
10. J.C.R. HUNT, Magnetohydrodynamic Flow in Rectangular Ducts, Journal of Fluid Mechanics, **21**, 577 (1965)
11. J.S. WALKER, Magnetohydrodynamic Flow in Rectangular Ducts with Thin Conducting Walls, J. Mécanique, **20**, 79 (1981)
12. R.J. MOREAU, Magnetohydrodynamics, Kluwer Academic Publishers (1990)
13. U. MŮLLER, L. BŮHLER, Magnetofluiddynamics in Channels and Containers, Springer (2001)
14. A. STERL, Numerical Simulation of Liquid-Metal MHD Flows in Rectangular Ducts, Journal of Fluid Mechanics, **216**, 161 (1990)
15. L. LEBOUCHER, Monotone Scheme and Boundary Conditions for Finite Volume Simulation of Magnetohydrodynamic Internal Flows at High Hartmann Number, Journal of Computational Physics, **150**, 181 (1999)
16. Y. SHIMOMURA, Large Eddy Simulation of Magnetohydrodynamics Turbulent Channel Flows under a Uniform Magnetic Field, Physics of Fluids A, **3**, 3098 (1991)
17. N. UMEDA, M. TAKAHASHI, Numerical Analysis for Heat Transfer Enhancement of a Lithium Flow under a Transverse Magnetic Field, Fusion Engineering and Design, **51-52**, 899 (2000)
18. C. MISTRANGELO, Three-Dimensional MHD Flow in Sudden Expansion, Ph.D Thesis, der Fakultät für Maschinenbau, der Universität Karlsruhe (2005)
19. I.D. PIAZZA, A General Computational Approach for Magnetohydrodynamic Flows Using the CFX Code: Buoyant Flow Through a Vertical Square Channel, Fusion Technology, **38** (2000)
20. S. ALEKSANDROVA, S. MOLOKOV, C.B. REED, Modeling of Liquid Duct and Free-Surface Flows Using CFX, ANL/TD/TM02-30 (2003)
21. M.-J. NI, M.A. ABDOU, Projection and SIMPLE Methods for Incompressible Flows with/without Phase Change, 13th International Heat and Mass Conference, Sydney, Australia, August 12-18, 2006
22. C.B. REED, B.F. PICOLOGLOU, T.Q. HUA, J.S. WALKER, ALEX Results – A Comparison of Measurements from a Round and a Rectangular Duct with 3-D Code Predictions, the 12th Symposium on Fusion Engineering, CA, Oct. 1267 (1987)
23. T.Q. HUA, J.S. WALKER, B.P. PICOLOGLOU, C.B. REED, Three-Dimensional MHD Flows in Rectangular Ducts in Nonuniform Transverse Magnetic Field Relevant to Fusion Blanket, Fusion Technology, **8**, 241 (1989)
24. R. MUNIPALLI, S. SHANKAR, M.-J. NI, N.B. MORLEY, Development of a 3-D Incompressible Free Surface MHD Computational Environment for Arbitrary Geometries: HIMAG", DOE SBIR Phase-II Final Report (2003)